An ATF2-derived peptide sensitizes melanomas to apoptosis and inhibits their growth and metastasis

Rapid Publication

Anindita Bhoumik,[1] Tian-Gui Huang,[2] Vladimir Ivanov,[1] Lisa Gangi,[3] Rui F. Qiao,[1] Savio L.C. Woo,[2] Shu-Hsia Chen,[2] and Ze'ev Ronai[1]

[1]Ruttenberg Cancer Center, and
[2]The Carl C. Icahn Institute for Gene Therapy and Molecular Medicine, Mount Sinai School of Medicine, New York, New York, USA
[3]Laboratory of Molecular Technology, National Cancer Institute–Science Applications International Corporation, Frederick, Maryland, USA

Melanomas are among the aggressive tumor types because of their notorious resistance to treatment and their high capacity to metastasize. ATF2 is among transcription factors implicated in the progression of melanoma and its resistance to treatment. Here we demonstrate that the expression of a peptide spanning amino acids 50–100 of ATF2 (ATF2$^{50–100}$) reduces ATF2 transcriptional activities while increasing the expression and activity of c-Jun. Altering the balance of Jun/ATF2 transcriptional activities sensitized melanoma cells to apoptosis, an effect that could be attenuated by inhibiting c-Jun. Inhibition of ATF2 via RNA interference likewise increased c-Jun expression and primed melanoma cells to undergo apoptosis. Growth and metastasis of SW1 and B16F10 mouse melanomas were inhibited by ATF2$^{50–100}$ to varying degrees up to a complete regression, depending on the mode (inducible, constitutive, or adenoviral delivery) of its expression. Thus, by attenuating ATF2 and inducing c-Jun activity, ATF2$^{50–100}$ inhibits melanoma growth and metastasis.

This article was published online in advance of the print edition.
The date of publication is available from the JCI website, http://www.jci.org.
J. Clin. Invest. **110**:643–650 (2002). doi:10.1172/JCI200216081.

Introduction

The growth and metastasis of melanoma together with its resistance to therapy present major obstacles to most conventional therapies. CREB, c-Jun, ATF1, ATF2, Stat3, and NF-κB are among transcription factors shown to play an important role in the course of melanoma development and progression (1–3). ATF2 has been found to play an important role in melanoma's proliferation (4) and resistance to treatment (1, 5). Attenuating the activities of ATF2 appears to be sufficient to sensitize melanoma to treatment (5, 6).

ATF2 is a member of the ATF/CREB protein family of basic-region leucine zipper (bZIP) proteins (7), which are involved in the response to stress (8). Transcriptionally active ATF2 recognizes and binds specific ATF/CRE motifs as a homo- or a heterodimer form (7, 8). Stimulation of ATF2 transcriptional activity can result from its phosphorylation by the stress kinases p38 or JNK (9), as well as from its interaction with any of several transcription factors, including c-Jun (10), NF-κB (11), and retinoblastoma protein (12). ATF2 has been implicated in the regulation of a wide set of genes that play roles in the regulation of cell growth, differentiation, immune response, and apoptosis, including c-*Jun* (8), TNF-α (13), TGF-β (12), cyclin A (14), and E-selectin (11). ATF2 has also been implicated in cellular proliferation in vitro and tumor formation in vivo through its cooperation with v-Jun (15). Similarly, c-Jun–ATF2 dimers have been implicated in oncogenesis (16).

Hypophosphorylated or transcriptionally inactive forms of ATF2 reduce TNF-α expression, resulting in sensitization of melanoma to treatment via increased apoptosis (5, 17). Screening of ATF2-driven peptides identified amino acids 50–100 (ATF2$^{50–100}$) as capable of sensitizing cultured melanoma cells to apoptosis induced by chemotherapeutic drugs, ribotoxic agents, or inhibitors of stress kinases (6). ATF2$^{50–100}$ contains the phosphoacceptor sites for JNK or p38, the binding domain for JNK (18), and has been implicated in p300-dependent transcriptional activation (19). Here we demonstrate using in vivo models that the ATF$^{50–100}$ peptide efficiently inhibits growth and metastasis of melanoma and sensitizes human and mouse melanoma tumors to treatment and points to the mechanism underlying ATF2 peptide's ability to elicit these effects.

Methods

Cells. SW1 and B16F10 mouse melanoma cells were maintained in DMEM supplemented with 10% FBS, L-glutamine, and antibiotics.

Constructs. ATF2 peptides were cloned in frame into a hemagglutin-penetratin (HA-penetratin) pcDNA3 vector (6). ATF2 peptide, corresponding to amino acids 50–100 of human ATF2, shares 100% homology with the murine sequence (corresponding amino acids in the mouse ATF2 cDNA are 33–82). Jun2-luciferase (Jun2-luc) and TRE-luc constructs were previously described (8, 10). The ATF2$^{50–100}$ peptide was

Received for publication June 5, 2002, and accepted in revised form July 9, 2002.

Address correspondence to: Ze'ev Ronai, The Ruttenberg Cancer Center, Mount Sinai School of Medicine, One Gustave L. Levy Place, Box 1130, New York, New York 10029, USA. Phone: (212) 659-5571; Fax: (212) 849-2425; E-mail: zeev.ronai@mssm.edu.

Conflict of interest: No conflict of interest has been declared.

Nonstandard abbreviations used: luciferase (luc); wild-type (WT); Fas ligand (FasL); TNF-related apoptosis inducing ligand (TRAIL); TRAIL receptor 1 (TRAIL-R1); β-galactosidase (β-gal); hemagglutin (HA); small interfering RNAs (RNAs).

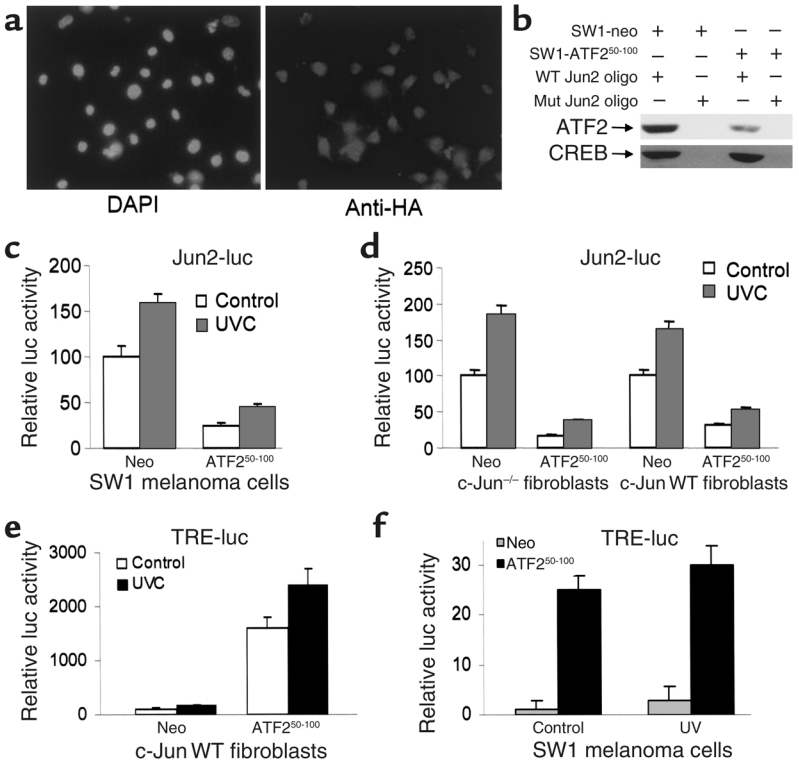

Figure 1

(**a**) Expression of the ATF2$^{50–100}$ peptide in SW1 cells. Mouse melanoma tumor-derived cells (SW1) were transfected with control or an HA-tagged ATF2$^{50–100}$ construct and clones were examined by immunohistochemistry using anti-HA antibodies. (**b**) Decreased ATF2 binding oligo bearing Jun2 motif in SW1 cells expressing ATF2$^{50–100}$ peptide. Nuclear proteins were incubated with biotinylated oligonucleotides bearing Jun2 motif. Oligo-bound proteins were captured on avidin-coated beads; then nonspecific bound proteins were removed by extensive washes, and bound material was subjected to analysis via Western blotting using antibodies to ATF2 and CREB. (**c**) Decreased Jun2-luc activity in SW1 mouse melanoma tumors expressing ATF2$^{50–100}$ peptide. SW1 cells that constitutively express control or ATF2$^{50–100}$ were transfected with the Jun2-luc and β-galactosidase (β-gal) constructs to monitor transcriptional activity of ATF2 and c-Jun. Proteins were assayed for β-gal activity and luciferase activity. Values depict relative luciferase activity normalized with respect to transfection efficiency based on β-gal assays. (**d**) Jun2-luc activity in Jun-null and WT cells. Shown is a Jun2-luc analysis similar to that shown in **c** except that the cell types used were Jun$^{+/+}$ or null mouse fibroblasts. (**e**) TRE-luc activities in mouse fibroblast cells. Analysis of TRE-luc activities was carried out as indicated in **c** using mouse fibroblast cells that carry WT Jun. (**f**) SW1 cells expressing ATF2 peptide exhibit increased TRE-luc activity. Control and ATF2 peptide–expressing SW1 cells were transfected with the TRE-luc and β-gal constructs, and degree of TRE-mediated transcriptional activity was measured. Values were normalized per β-gal activity. DAPI, 4,6-diamino-2 phenylindole dilactate; UVC, ultraviolet-c radiation; neo, neomycin.

cloned in frame with HA and penetratin into the SpeI and NotI sites in the PadL1-RSV-BPA vector (20). For the doxycycline-inducible system the ATF2$^{50–100}$ peptide was cloned in frame with HA and penetratin into SacII and XbaI sites of the PUHD10-3 vector (21). The PeF1PrtTA vector (22) places the rtTA gene under transcriptional control of the human EF-1α promoter. Replication-deficient adenovirus expressing ATF2$^{50–100}$ was generated by subcloning the ATF2 peptide cDNA into the corresponding adenovirus vector as previously described (20).

Cell culture and derivation of stable cell line. Selection of clones stably expressing the rtTA construct was carried out in SW1 cells in the presence of 600 μg/ml of G418. After the selection period, we picked and expanded 12 single colonies and analyzed them for activity by assaying for luciferase activity (22). The clone that exhibited eightfold induction upon addition of doxycycline was chosen. The positive clone, which expresses the rtTA cDNA, was cotransfected with PUHD10-3 ATF2$^{50–100}$ and pBabe Puro, and single clones were selected with 2 μg/ml of Puromycin.

Transcriptional analysis. Transient transfection of different reporter constructs (0.5 μg) with expression vectors and pCMV-βgal (0.1 μg) into 5×10^5 melanoma cells was performed using Lipofectamine (Life Technologies Inc., Carlsbad, California, USA). Luciferase activity was determined as previously described (23).

RNA interference. RNAs of 21 nucleotides (24), designed to target mouse ATF2 within nucleotides 119–135 (sense: 5′-AGCACGUAAUGACAGUGUCTT-3′; antisense: 5′- GACACUGUCAUUACGUGCUTT-3′), were synthesized, deprotected, and HPLC-purified (Midland Certified Reagent Co., Midland, Texas, USA). For annealing of small interfering RNAs (siRNAs), 20 μM single strands were incubated in annealing buffer (100 mM potassium acetate, 30 mM HEPES-KOH at pH 7.4, 2 mM magnesium acetate) for 1 minute at 90°C followed by 1 hour at 37°C. siRNAs were transfected into SW1 cells (2.4 μg siRNA duplex per six-well plate) using Lipofectamine (Life Technologies Inc.). siRNAs of RNF5, a RING finger protein important in cytoskeleton organization (our unpublished studies), were used as control.

Treatment and apoptosis studies. Cells were exposed to concentrations of the chemicals (10 μM UCN-01-7-hydroxystaurosporine [UCN-01], 500 μg/ml neocarzinostatin [NCS], 10 μg/ml anisomycin) or of the pharmacological inhibitors (50 μM LY294002, an inhibitor of phosphatidylinositol [PI] 3-kinase; 50 μM PD98059, an inhibitor of mitogen-activated protein kinase [MAPK]; 50 μM AG490, an inhibitor of JAK; 10 μM SB203580, an inhibitor of p38/JNK) for 36 hours; then FACS analysis was carried out to measure the hypodiploid cell populations. Apoptosis was assessed by quantifying the percentage of hypodiploid nuclei undergoing DNA fragmentation to the left of the diploid $G_{0/1}$ peak (17).

Western blot analysis and immunohistochemistry. Cell lysates (50–100 μg protein) were resolved on 10% SDS-PAGE, transferred to nitrocellulose,

and processed according to the standard protocols. The antibodies used were polyclonal anti-ATF2, phospho-ATF2, c-Jun, phospho–c-Jun (NEB), and anti-HA (BaBco). The primary antibodies were used at dilutions of 1:1,000 to 1:3,000. The secondary antibodies were anti-rabbit or anti-mouse IgG conjugated to horseradish peroxidase (dilution 1:5,000). Signals were detected using ECL (Amersham Life Sciences Inc., New Wark, New Jersey, USA). Immunoprecipitation was carried out by standard methods.

Tumor growth and metastasis in vivo. SW1 cells that express control or ATF2$^{50–100}$ peptide were trypsinized, resuspended in PBS, and injected subcutaneously (1×10^6) into 6- to 7-week-old mice in the lower flank. Tumor growth was monitored every 2 days. SW1 cells expressing the tet-inducible ATF2$^{50–100}$ peptide were injected subcutaneously (1×10^6). When tumors reached a size of about 50 mm^3, the mice received doxycycline in their drinking water (500 μg/ml). At the end of the experiment, the tumors were excised and weighed. To detect metastatic lesions, the lungs as well as other organs were subjected to histopathological examination. In the case of adenoviral injection, SW1 cells were injected subcutaneously to groups of 12 mice per experimental condition, and tumors reached the size of 40 mm^3 before virus control, solution control, or virus carrying the ATF2 peptide was first injected (1.5×10^{10} virus particles per intratumoral injection). A second injection took place 4 days later. Tumors were measured for up to 3 weeks. C57BL/6 mice (12 mice per group in one set of experiments and 6 mice per group in a second experiment) were injected with B16F10 cells (2×10^5, subcutaneously), and tumors grew to the size of 40 mm^3 before injections of adenovirus bearing the ATF2 or control construct were initiated. Virus injection (1.5×10^{10} virus particles per injection) took place three times at the time points indicated in the figures.

Histology analysis and immunohistochemistry. Tissue samples were fixed in formalin and embedded in paraffin. Hematoxylin and eosin staining, TUNEL staining, and immunohistochemistry for HA were performed as previously described (6).

Results

The ATF2$^{50–100}$ peptide alters transcriptional activities of ATF2 and c-Jun. SW1 cells, derived from mouse melanoma, which is highly tumorigenic and metastatic (25), were transfected with ATF2$^{50–100}$–expressing vector, and cell populations that exhibited constitutive expression of this peptide or control vector were selected (Figure 1a). Binding of ATF2 to oligonucleotide bearing Jun2 motif was reduced in nuclear extracts prepared from ATF2$^{50–100}$–expressing SW1 cells, whereas there was no effect on the binding of CREB (Figure 1b). Analysis of the Jun2-luc reporter gene revealed a fivefold decrease in basal as well as ultraviolet-inducible levels of Jun2-dependent transcriptional activities in SW1 cells that constitutively express the ATF2$^{50–100}$ peptide (Figure 1c). These findings suggest that ATF2$^{50–100}$ interferes with endogenous ATF2 and/or c-Jun transcriptional activities. Expression of the ATF2$^{50–100}$ peptide also decreased basal as well as ultraviolet-inducible levels of Jun2-luc activities in wild-type (WT) as well as in Jun-null fibroblasts, similar to what was observed in the SW1 melanoma cells (Figure 1d).

Whereas the oligonucleotides bearing Jun2 motif primarily bind ATF2/Jun heterodimers, the TRE motif interacts with c-Jun/c-Fos as well as with other members of the AP1 family (8, 10, 26). Analysis of TRE-luc in ATF2 peptide–expressing fibroblasts revealed a remarkable increase in the

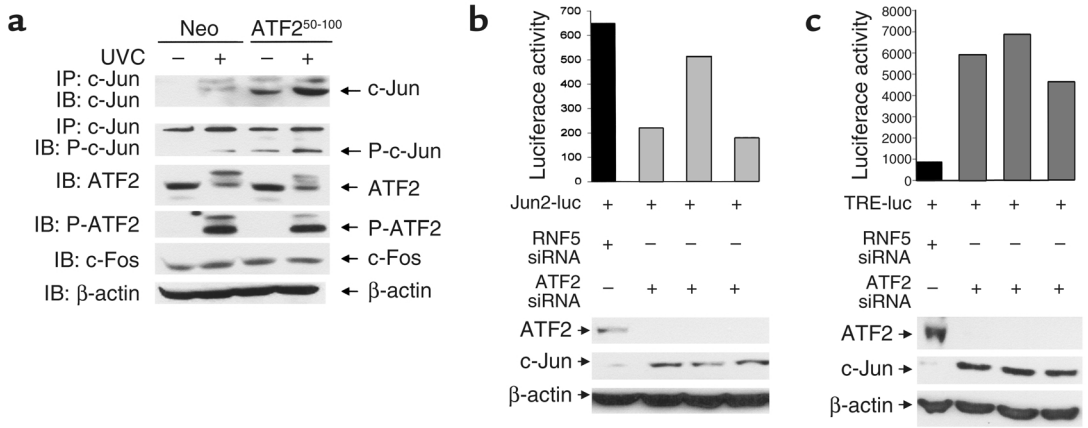

Figure 2

(**a**) Expression of ATF2$^{50–100}$ increases expression of c-Jun. Protein extracts prepared from indicated cells were subjected to immunoprecipitation with antibodies to c-Jun followed by immunoblot analysis using antibodies to phosphorylated c-Jun or control non-phosphoantibodies. Parallel analysis was carried out using antibodies to ATF2, c-Fos, and β-actin. Slow-migrating bands in ATF2 Western blots are likely to represent covalently modified forms of ATF2. (**b**) ATF2-siRNA alters c-Jun and ATF2 expression and the activity of Jun2-luc. SW1 cells were cotransfected with ATF2-siRNA and Jun2-luc as well as β-gal constructs. A portion of the same transfectants was taken for analysis of ATF2 and c-Jun expression to confirm inhibition of ATF2 by siRNA (lower panels). Luciferase assays carried out to monitor changes in TRE-mediated transcription are indicated following their normalization to β-gal. For the three experiments shown, $P = 0.0167$. (**c**) ATF2-siRNA alters c-Jun and ATF2 expression and the activity of TRE-luc. Experiment was performed as indicated in panel **b**, except that TRE-luc was used. For the three experiments shown, $P = 0.0027$. P-ATF2, phospho-ATF2; P-c-Jun, phospho-c-Jun.

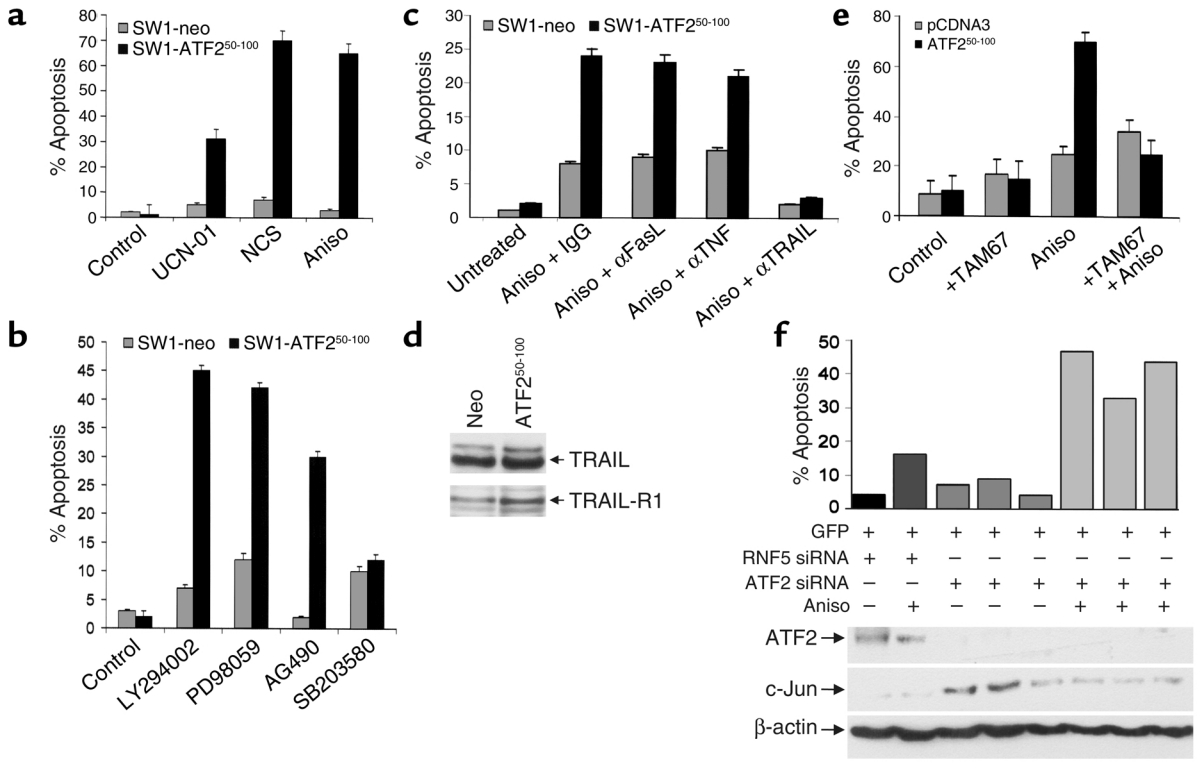

Figure 3

(**a**) Sensitization of ATF2$^{50–100}$ peptide–expressing SW1 melanoma cells to apoptosis. SW1 cells expressing the ATF2$^{50–100}$ peptide or control peptide were treated with the indicated drugs, followed by FACS analysis to measure the hypodiploid cell populations. (**b**) Sensitization of SW1 melanoma to apoptosis by inhibitors of specific signaling pathways. SW1 cells expressing the ATF2$^{50–100}$ peptide were treated with the pharmacological inhibitors indicated, followed by FACS analysis to reveal the percentage of apoptotic cells. (**c**) Inhibition of TRAIL abolishes sensitivity of ATF2$^{50–100}$–expressing SW1 cells to anisomycin-induced apoptosis. Control and ATF2$^{50–100}$–expressing SW1 cells were pretreated with neutralizing antibodies to FasL, TRAIL, or TNF. Twenty-four hours later, cells were subjected to anisomycin (Aniso) treatment, and degree of apoptosis was monitored via FACS analysis. (**d**) ATF2$^{50–100}$–expressing cells exhibit an increase in expression of TRAIL receptor. Western blot analysis using antibodies to TRAIL or TRAIL receptor 1 was performed on extracts prepared from the indicated cells. (**e**) Dominant negative c-Jun construct attenuates the sensitivity of SW1 cells to anisomycin-induced apoptosis. Control cells and SW1 cells expressing ATF2 peptide were transfected with a dominant negative form of c-Jun (TAM67), and cells were subjected to anisomycin treatment. Degree of apoptosis was monitored via FACS analysis. (**f**) ATF2-siRNA sensitizes SW1 cells to apoptosis. Cotransfection of ATF2-siRNA and green fluorescent protein was followed by treatment of cells with anisomycin and analysis of green fluorescent protein–positive cells for apoptosis via FACS. For the three experiments shown, $P = 0.0039$. UCN-01, UCN-01-7-hydroxystaurosporine; NCS, neocarzinostatin.

activities of TRE-luc (Figure 1e). Similarly, expression of the ATF2 peptide led to a marked increase in basal TRE-luc activities in the SW1 cells (Figure 1f). These data suggest that expression of the ATF2 peptide suffices to increase transcriptional activities of the c-Jun or Jun family members that recognize the AP1 target sequence.

The ATF2$^{50–100}$ peptide or inhibition of ATF2 increases c-Jun expression and activity. Expression of ATF2$^{50–100}$ did not alter the phosphorylation or expression of endogenous ATF2 (Figure 2a). In contrast, ATF2$^{50–100}$–expressing cells exhibit a noticeable increase in the level of c-Jun protein (Figure 2a), which coincides with increased TRE-mediated transcription (Figure 1, e and f). To determine the possible mechanism underlying the marked increase in expression and activity of c-Jun, we have assessed whether inhibition of ATF2 expression per se (which would result in decreased ATF2-mediated transcription as seen in ATF2 peptide–expressing cells; Figure 1, c and d) would suffice to increase c-Jun expression and activities. Using ATF2-siRNA oligonucleotides, we have generated a transient ATF2-null environment in the SW1 melanoma cells. Transfection of ATF2-siRNA resulted in efficient inhibition of ATF2 and an increase in c-Jun RNA transcripts as revealed by RT-PCR (data not shown). SW1 cells transfected with ATF2-siRNA also exhibited increased c-Jun and decreased ATF2 expression at the protein levels (Figure 2, b and c). These data suggest that inhibition of ATF2 expression suffices to increase c-Jun transcription and expression in the melanoma cells studied here, similar to the effect of the ATF2 peptide used in the present studies.

We next assessed whether the increase in c-Jun expression would also be reflected in its transcriptional activities. Measurement of Jun2-luc in ATF2-siRNA–expressing cells revealed inhibition of Jun2-mediated transcription that coincided with the degree of decreased ATF2 and increased c-Jun expression (Figure 2b). In contrast to inhibition of Jun2-luc activity, expression of ATF2-siRNA caused a noticeable increase in TRE-mediated transcription (Figure 2c).

These data indicate that the inhibition of ATF2 expression suffices to

increase c-Jun expression, resulting in elevated TRE-based transcription while attenuating Jun2-based transcription. As these changes resemble the effects upon the expression of ATF2$^{50–100}$ peptide, these findings suggest that the primary mechanism underlying the changes monitored in the melanoma cells upon expression of the ATF2$^{50–100}$ peptide could be attributed to the inhibition of ATF2 activity. Neither JNK nor p38 was found to be capable of phosphorylating the ATF2$^{50–100}$ peptide in vitro (data not shown). This suggests that inhibition of ATF2 activities may be mediated by the peptide's ability to interfere with ATF2 binding and/or assembly of the transcription initiation complex.

Using GST-ATF2$^{50–100}$, we found that the ATF2 peptide binds to ATF2 but not to c-Jun. Further, JNK was also bound to the GST-ATF2$^{50–100}$ peptide (data not shown), which is in line with former studies indicating that JNK association with ATF2 requires amino acids 40–60 of ATF2 (18) and critical residues within the 51–100 peptide (Nic Jones, personal communication).

Mouse melanoma cells expressing the ATF2$^{50–100}$ peptide are sensitized to TNF-related apoptosis inducing ligand–mediated apoptosis. Expression of the ATF2$^{50–100}$ peptide in SW1 cells resulted in a profound degree of apoptosis (6- to 14-fold increase) after treatment with chemotherapeutic, ribotoxic, or radiomimetic drugs (Figure 3a). Similarly, ATF2$^{50–100}$–expressing cells exhibited a marked increase (four- to ten-fold) in the degree of apoptosis following treatment with inhibitors of JAK, MAPK, and PI 3-kinase signaling cascades (Figure 3b). These observations indicate that expression of the ATF2 peptide suffices to sensitize melanoma cells to treatments that otherwise do not affect this tumor type.

To identify the apoptotic pathway that sensitized ATF2 peptide–expressing SW1 cells to treatment, these cells were treated with antibodies that neutralize TNF-related apoptosis inducing ligand (TRAIL), Fas ligand (FasL), or TNF-α, respectively, thereby inactivating the corresponding death pathways. Only the neutralization of TRAIL reduced (from 22% to 2%) anisomycin-induced apoptosis of ATF2 peptide–expressing SW1 cells (Figure 3c). Treatment of SW1 cells with TRAIL in the presence of cycloheximide led to a marked increase in degree of apoptosis of cells that express the ATF2 peptide (data not shown). These results demonstrate that expression of the ATF2 peptide changed the apoptotic cascade toward the TRAIL pathway. Western blot analysis did not reveal changes in the level of TRAIL but identified increase in the expression of TRAIL receptor 1 (TRAIL-R1) in SW1 cells that express ATF2$^{50–100}$ peptide (Figure 3d), providing a plausible explanation for their greater sensitivity to apoptosis upon various stimuli.

To directly assess whether elevated c-Jun expression and activities are the primary cause of melanoma sensitization to treatment, we used a dominant negative form of c-Jun (TAM67) (27). Forced expression of TAM67 abolished ATF2$^{50–100}$–expressing SW1 cells' ability to undergo apoptosis in response to anisomycin treatment (Figure 3e). These results provide

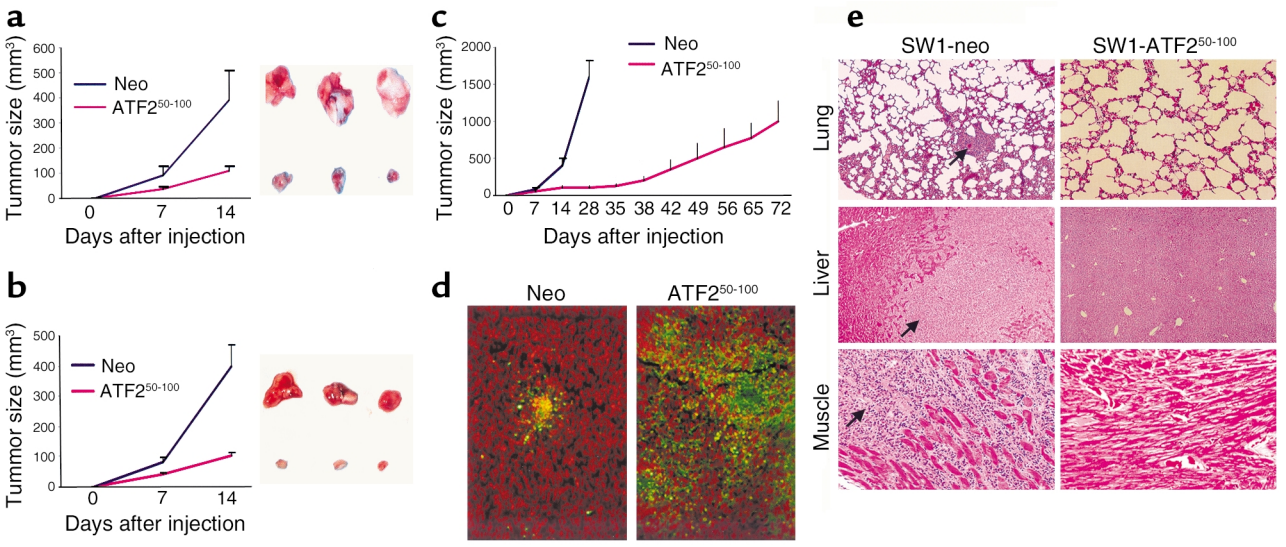

Figure 4

(**a**) Mouse melanoma expressing the ATF2$^{50–100}$ peptide grow to a substantially smaller size. SW1 cells that express control vector or the ATF2$^{50–100}$ peptide were injected subcutaneously into C3H/HEJ mice, and tumor growth was monitored. The right panel depicts representative tumors at the end of the study, and the left panel shows tumor growth. The experiment was repeated three times. Bars = SD; $P < 0.0001$. (**b**) SW1 cells that express empty vector or the ATF2$^{50–100}$ peptide were injected subcutaneously into C3H/GLD (GLD mice bear mutations in FasL) mice, and follow-up and analysis were performed as indicated in **a**. Bars = SD; $P < 0.0001$. (**c**) Long-term growth of tumors from ATF2$^{50–100}$ peptide–expressing SW1 cells in C3H/HEJ mice. Tumors were measured at the indicated time points. Bars = SD; $P < 0.0003$. (**d**) Apoptosis of SW1 tumors expressing the ATF2$^{50–100}$ peptide. Sections of SW1 tumors produced in the presence of ATF2$^{50–100}$ peptide or control vector, tested for apoptosis by the TUNEL assay (apoptotic cells are green). (**e**) Expression of the ATF2$^{50–100}$ peptide in SW1 cells inhibits metastasis. Mice bearing tumors produced by cells that constitutively express the ATF2$^{50–100}$ peptide were monitored for metastatic lesions in the indicated organs at the end of inoculation. Arrows point to the metastatic lesions seen in the control group at the end of their inoculation.

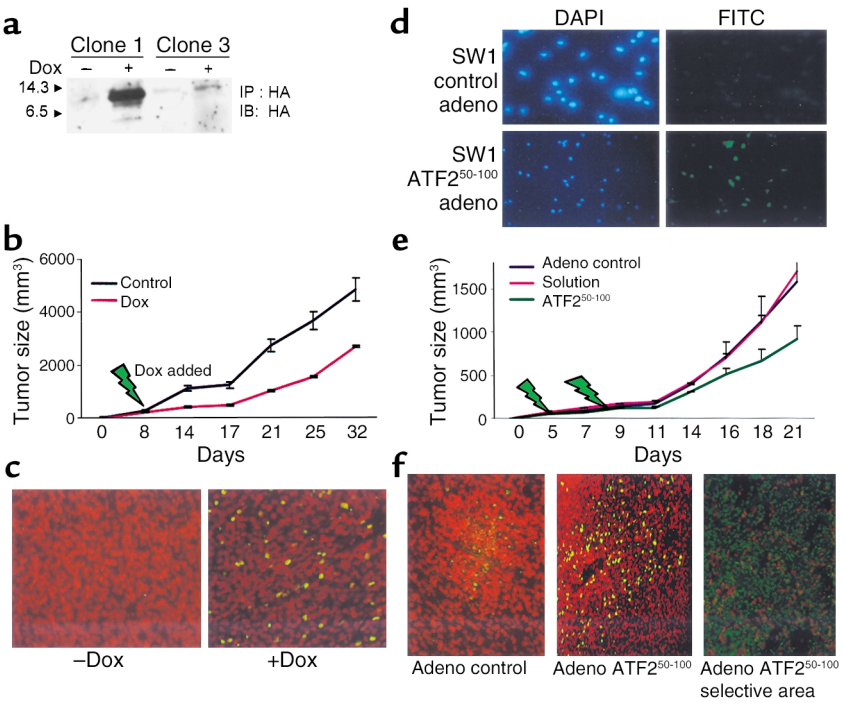

Figure 5

Administration of ATF2$^{50–100}$ peptide to existing SW1 tumors reduces their growth in C3H mice. (**a**–**c**) SW1 cells that exhibit inducible expression of the ATF2$^{50–100}$ peptide following addition of doxycycline were selected (**a**) and injected (clone 1) into C3H mice. Eight days after inoculation, doxycycline was added to the drinking water. Tumors were measured at the indicated times (**b**; $P < 0.003$). Analysis of apoptosis via the TUNEL assay revealed marked apoptosis in the tumors obtained from doxycycline-treated mice (**c**, green staining). (**d**) SW1 cells were infected with adenovirus (adeno) control or with adenovirus that expresses ATF2$^{50–100}$ peptide, and then subjected to immunohistochemistry analysis using antibodies to HA (HA is cloned in frame with the ATF2 peptide sequence). Left panels depict DAPI staining, whereas right panels show the fluorescence upon positive staining with HA antibodies. (**e**) SW1 cells were injected subcutaneously and tumors reached the size of 40 mm^3 before virus control, solution control, or virus carrying the ATF2 peptide was injected (green arrows indicate injection). Data shown represent two experiments. $P < 0.02$ between control virus and the ATF2 peptide adenovirus groups. (**f**) Analysis of tumors for apoptosis via the TUNEL assay. Comparable magnification of control virus and ATF2 virus is shown in the two left panels; the right panel depicts a selective area representative of marked apoptosis within focal areas, seen in tumors that express the ATF2 peptide.

direct evidence for the role of c-Jun in mediating the sensitization of melanoma cells to apoptosis following expression of the ATF2$^{50–100}$ peptide. To further assess the role of ATF2 versus c-Jun in the sensitization of melanoma cells to treatment, we monitored sensitivity to apoptosis of cells that were transfected with ATF2-siRNA. Transient null ATF2 environment generated upon transfection of the ATF2-siRNA was sufficient to sensitize the SW1 melanoma cells to apoptosis in response to anisomycin treatment (Figure 3f). The degree of apoptosis seen in cells transfected with ATF2-siRNA was threefold higher than that seen using siRNA of RNF5, a RING finger protein involved in cytoskeleton organization (our unpublished data), which was used here as a control. These findings indicate that changes elicited upon inhibition of ATF2 expression in the melanoma cells are sufficient to cause their sensitization to apoptosis upon treatment, as has been observed with the ATF2 peptide–expressing cells.

Expression of ATF2$^{50–100}$ in SW1 mouse melanoma cells causes marked reduction in their growth and inhibits their metastatic capacity. Subcutaneous injection of SW1 cells expressing a control construct resulted in rapid growth producing 400-mm^3 tumors within 2 weeks. Tumors produced by SW1 cells that constitutively express the ATF2$^{50–100}$ peptide were much smaller (90 mm^3; Figure 4a). The expression of the ATF2$^{50–100}$ peptide was as efficient in blocking growth of SW1 tumors in FasL-deficient *GLD* mice (Figure 4b), suggesting that the sensitization of the ATF2$^{50–100}$–expressing tumors to apoptosis is not dependent on the exogenous source of FasL.

While the parental cells produced tumors weighing about 1 g within 28 days after inoculation, it took 72 days (three times longer) for ATF2$^{50–100}$–expressing cells to produce similar-sized tumors (Figure 4c). The strongest inhibition of growth was observed during the first 35 days after inoculation, with somewhat increased growth rate thereafter. The partial loss of growth inhibition could be attributed to a selective loss of the ATF2$^{50–100}$ peptide due to lack of selective pressure (to maintain drug resistance) and lack of genomic integration of the plasmid vector. While Western blot analysis confirmed expression of ATF2 peptide, immunohistochemistry analysis revealed focal expression (data not shown), which coincided with foci of apoptotic cells as seen via the TUNEL assay (Figure 4d), thereby confirming partial expression of the ATF2 peptide at this stage.

SW1 cells are prone to metastasize into multiple organs, resulting in multiple lesions as early as 4 weeks following injection (25); however, no metastasis was seen in experiments where ATF2$^{50–100}$–expressing SW1 cells were monitored for up to 72 days (Figure 4e).

Inducible expression of the ATF2$^{50–100}$ peptide suffices to attenuate growth of SW1 tumors. To explore whether expression of this peptide in existing tumors would affect their growth, we generated SW1 cells in which the expression of the ATF2$^{50–100}$ peptide is induced upon addition of doxycycline (Figure 5a). Following the inoculation of these modified SW1 cells, when tumors reached the size of 50 mm^3, the expression of ATF2 peptide was induced, and maintained by adding doxycycline to the drinking water for 24 days. Inducible expression of ATF2 after tumor formation resulted in a twofold decrease in the growth of SW1 tumors (Figure 5b). Tumors excised from doxy-

cycline-fed mice exhibited an increase in degree of apoptosis, albeit sporadic (Figure 5c), which coincides with partial expression of the ATF2$^{50–100}$ peptide as revealed by immunohistochemistry of the tumors (not shown).

In a parallel approach, the cDNA of the ATF2 peptide was cloned into an adenovirus vector and administered to SW1 tumors (40 mm^3 in size) via direct intratumoral injection. Expression of adenovirus encoding the ATF2$^{50–100}$ peptide was confirmed via immunofluorescence (Figure 5d). A marked reduction (~50%) in tumor growth was observed shortly after the second adenoviral injection (Figure 5e). Inhibition of tumor growth coincided with elevated degree of apoptosis, which was nonhomogenous (Figure 5f). These data suggest that partial expression of the ATF2$^{50–100}$ peptide in already developed melanoma suffices to elicit efficient reduction of subsequent tumor growth.

Regression of B16F10 melanoma following injection of the ATF2$^{50–100}$ peptide. Injection of adenovirus bearing the ATF2$^{50–100}$ peptide into 18 B16F10 tumors that had reached the size of 40 mm^3 had no effect on four tumors (22%) but caused complete regression in seven (39%) and reduced the growth of seven (Figure 6, a and c). Importantly, 14 of 18 animals injected with the ATF2$^{50–100}$ peptide had no metastatic lesions as opposed to the parent tumors (Figure 6b). Survival and percentage of tumor-free animals were higher in the group treated with the ATF2$^{50–100}$ peptide; about 50% of ATF2 peptide–expressing mice survived after 70 days, compared with less than 10% of the control adenovirus group (Figure 6d). These findings suggest that in vivo administration of the peptide via an adenovirus vector results in efficient inhibition of growth extending up to a complete regression of B16F10 tumors. Interestingly, multiple administration of the adenovirus vector alone was sufficient to cause some decrease in growth and increased survival, probably because of the known adjuvant-like effect generated by multiple injections of adenovirus.

Discussion

The study presented here demonstrates, using two different model systems and three different modes of expression, the ability of a 51–amino acid peptide derived from the ATF2 transactivating domain to alter melanoma growth and metastasis capacity in vivo. Further, expression of ATF2 peptide in human melanoma cell lines also inhibited their growth in nude mice (data not shown). The efficiency of the ATF2$^{50–100}$ peptide appears to be dependent on the genetic and epigenetic background of the tumor to which it is targeted and of the host to which it was injected, as well as on its mode of administration. Whereas adenoviral delivery of the ATF2$^{50–100}$ peptide resulted in a complete regression in some of the B16F10 tumors, it caused only 50% inhibition in the growth of SW1 tumors. Similarly, constitutive expression of the ATF2 peptide led to almost complete inhibition of mouse SW1 tumor growth for the first 35 days. Changes in the effectiveness of the ATF2 peptide could also be attributed to alteration of the immune response, due either to the immunogenicity of the different tumors or to changes elicited by the peptide that may trigger better immune recognition.

The sensitization of melanomas to apoptosis points to an important advance in treatment of these tumors by reagents that otherwise do not affect this tumor type. It is expected that the effects of the ATF2 peptide on tumor growth rate and metastasis would be improved by combining the peptide with other treatments, including inhibitors of stress kinases, immunological modulators, or chemotherapeutic drugs, all of which efficiently induced apoptosis in vitro.

Inhibition of ATF2 activities in ATF2 peptide–expressing cells could stem from the association of the peptide with ATF2 (data not shown), since the peptide can interfere with its binding and/or overall transcriptional assembly. The marked increase in Jun expression and activities can be attributed to increased transcription of c-Jun upon inhibition of ATF2 expression. This observation points to the possible existence of a negative feedback loop between ATF2 and c-Jun in the melanoma cells studied here.

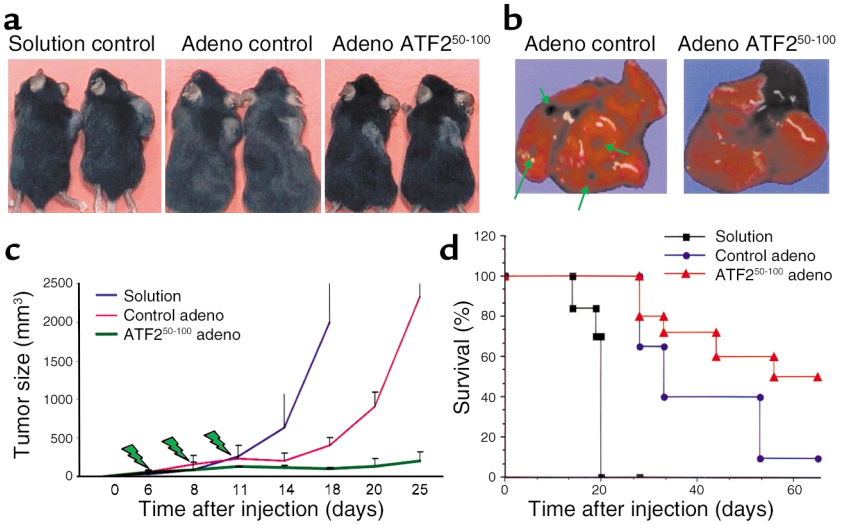

Figure 6

Intratumoral injection of adenovirus bearing the ATF2 peptide causes reduction of growth as well as complete regression of B16F10 tumors. C57BL/6 mice were injected with B16F10 cells, and tumors grew before injections of adenovirus bearing the ATF2 or control construct were initiated. Virus injection took place at the time points indicated in **c** (green arrows). (**a**) Representative tumors developed under each of the protocols. (**b**) The ATF2 peptide inhibited metastasis of the tumors. Green arrows point to metastatic lesions in the lungs seen in the control but not the treatment group; the black area in the photograph of ATF2 peptide–expressing mice depicts the heart. (**c**) Overall changes in the growth rate of the tumors subjected to control or ATF2 peptide treatments (compiled from the two experiments). Comparisons between all experimental groups are significant ($P < 0.0001$) as calculated by Tukey's multiple comparisons (Tukey's honestly significant difference). (**d**) The effect of ATF2 peptide on the survival of the mice under each of the protocols used.

Decreased ATF2 transcriptional activities together with a concomitant increase in c-Jun transcriptional activities is likely to be the primary mechanism underlying the observed effects upon the expression of the $ATF2^{50–100}$ peptide. This conclusion is supported by an independent set of experiments where siRNA used to inhibit ATF2 transcription resulted in increased c-Jun expression, transcription, and sensitization to apoptosis. The ability to abolish the sensitization of $ATF2^{50–100}$–expressing SW1 cells to anisomycin-induced apoptosis upon expression of a potent c-Jun dominant negative construct supports the central role of c-Jun, in conjunction with decreased ATF2 transcriptional activities, in the sensitization of melanoma cells to apoptosis. Of interest, increase in expression of TRAIL-R1 in ATF2 peptide–expressing cells could also be attributed to c-Jun, which was recently shown to positively regulate TRAIL-R promoter (28). The ability of c-Jun to induce apoptosis has been documented in several systems (29–31).

Support for the possible antioncogenic activities of c-Jun comes from the independent finding that c-Jun is capable of inhibiting oncogene-dependent in vitro transformation of primary rat embryo fibroblasts (32). Our findings are in agreement with these studies, as they point to the central role of c-Jun in sensitization of melanoma to apoptosis in conjunction with decreased ATF2 transcriptional activities. Accordingly, our findings suggest that the oncogenic activities of c-Jun may depend on its cooperation with other transcription factors, as demonstrated here for ATF2. In the absence of such cooperation there is a switch in the profile of c-Jun–regulated genes, as reflected in expression profiling analysis, which revealed an increase in TNF-α and a decrease in growth-, Fas-, and IFN-γ–related genes (data not shown).

Independent support for the role of ATF2 in proliferation of melanomas was recently provided in an HGF-based melanoma model (4). Overall, our results highlight the ability to "reprogram" c-Jun/ATF2 transcriptional activities via a 51–amino acid ATF2-driven peptide, resulting in the sensitization of melanoma to apoptosis and in the inhibition of the growth and metastasis of this otherwise aggressive tumor type.

Acknowledgments

We thank M. Herlyn and O. Fodstad for providing the melanoma cell lines, Ron Wisdom for the Jun-null cells, and Raul Gopalkrishnan and Paul Fisher for the doxycycline-inducible constructs. We also thank Lilliana Ossowski for critical reading, and John Mandeli for biostatistics analysis. We thank Nic Jones and members of the Ronai laboratory for discussions. Support by National Cancer Institute grant CA-59008 and CA-78419 (to Z. Ronai) and by the Sharp Foundation (to Z. Ronai and S.-H. Chen) is gratefully acknowledged.

1. Yang, Y.M., Dolan, L.R., and Ronai, Z. 1996. Expression of dominant negative CREB reduces resistance to radiation of human melanoma cells. *Oncogene.* **12**:2223–2233.
2. Jean, D., Harbison, M., McConkey, D.J., Ronai, Z., and Bar-Eli, M. 1998. CREB and its associated proteins act as survival factors for human melanoma cells. *J. Biol. Chem.* **273**:24884–24890.
3. Yang, J., and Richmond, A. 2001. Constitutive IkappaB kinase activity correlates with nuclear factor-kappaB activation in human melanoma cells. *Cancer Res.* **61**:4901–4909.
4. Recio, J.A., and Merlino, G. 2002. Hepatocyte growth factor/scatter factor activates proliferation in melanoma cells through p38 MAPK, ATF-2 and cyclin D1. *Oncogene.* **21**:1000–1008.
5. Ronai, Z., et al. 1998. ATF2 confers radiation resistance to human melanoma cells. *Oncogene.* **16**:523–531.
6. Bhoumik, A., Ivanov, V.N., and Ronai, Z. 2001. Activating transcription factor 2-derived peptides alter resistance of human tumor cell lines to ultraviolet irradiation and chemical treatment. *Clin. Cancer Res.* **7**:331–342.
7. Hai, T.W., Liu, F., Coukos, W.J., and Green, M.R. 1989. Transcription factor ATF cDNA clones: an extensive family of leucine zipper proteins able to selectively form DNA-binding heterodimers. *Genes Dev.* **3**:2083–2090.
8. van Dam, H., et al. 1995. ATF-2 is preferentially activated by stress-activated protein kinases to mediate c-jun induction in response to genotoxic agents. *EMBO J.* **14**:1798–1811.
9. Gupta, S., Campbell, D., Derijard, B., and Davis, R.J. 1995. Transcription factor ATF2 regulation by the JNK signal transduction pathway. *Science.* **267**:389–393.
10. van Dam, H., et al. 1993. Heterodimer formation of cJun and ATF-2 is responsible for induction of c-jun by the 243 amino acid adenovirus E1A protein. *EMBO J.* **12**:479–487.
11. Kaszubska, W., et al. 1993. Cyclic AMP-independent ATF family members interact with NF-kappa B and function in the activation of the E-selectin promoter in response to cytokines. *Mol. Cell. Biol.* **13**:7180–7190.
12. Kim, S.J., et al. 1992. Retinoblastoma gene product activates expression of the human TGF-beta 2 gene through transcription factor ATF-2. *Nature.* **358**:331–334.
13. Tsai, E.Y., Jain, J., Pesavento, P.A., Rao, A., and Goldfeld, A.E. 1996. Tumor necrosis factor alpha gene regulation in activated T cells involves ATF-2/Jun and NFATp. *Mol. Cell. Biol.* **16**:459–467.
14. Shimizu, M., et al. 1998. Activation of the rat cyclin A promoter by ATF2 and Jun family members and its suppression by ATF4. *Exp. Cell Res.* **239**:93–103.
15. Huguier, S., Baguet, J., Perez, S., van Dam, H., and Castellazzi, M. 1998. Transcription factor ATF2 cooperates with v-Jun to promote growth factor-independent proliferation in vitro and tumor formation in vivo. *Mol. Cell. Biol.* **18**:7020–7029.
16. van Dam, H., and Castellazzi, M. 2001. Distinct roles of Jun. Fos and Jun: ATF dimers in oncogenesis. *Oncogene.* **20**:2453–2464.
17. Ivanov, V.N., and Ronai, Z. 1999. Down-regulation of tumor necrosis factor alpha expression by activating transcription factor 2 increases UVC-induced apoptosis of late-stage melanoma cells. *J. Biol. Chem.* **274**:14079–14089.
18. Fuchs, S.Y., Dolan, L.R., Davis, R., and Ronai, Z. 1996. Phosphorylation dependent targeting of c-jun ubiquitination by Jun N-kinase. *Oncogene.* **13**:1531–1535.
19. Duyndam, M.C., et al. 1999. The N-terminal transactivation domain of ATF2 is a target for the cooperative activation of the c-jun promoter by p300 and 12S E1A. *Oncogene.* **18**:2311–2321.
20. Chen, S.H., Shine, H.D., Goodman, J.C., Grossman, R.G., and Woo, S.L. 1994. Gene therapy for brain tumors: regression of experimental gliomas by adenovirus-mediated gene transfer in vivo. *Proc. Natl. Acad. Sci. USA.* **91**:3054–3057.
21. Gossen, M., and Bujard, H. 1992. Tight control of genen expression in mammalian cells by tetracycline-responsive promoters. *Proc. Natl. Acad. Sci. USA.* **89**:5547–5551.
22. Gopalkrishnan, R.V., Christiansen, K.A., Goldenstein, N.I., DePinho, R.A., and Fisher, P.B. 1999. Use of the human EF-1alpha promoter for expression can significantly increase success in establishing stable cell lines with consistent expression: a study using the tetracycline-inducible system in human cancer cells. *Nucleic Acids Res.* **27**:4775–4782.
23. Ivanov, V.N., et al. 2001. Cooperation between STAT3 and c-jun suppresses Fas transcription. *Mol. Cell.* **7**:517–528.
24. Elbashir, S.M., et al. 2001. Duplexes of 21-nucleotide RNAs mediate RNA interference in cultured mammalian cells. *Nature.* **411**:494–498.
25. Owen-Schaub, L.B., van Golen, K., Hill, L., and Price, J.E. 1998. Fas and Fas ligand interactions suppress melanoma lung metastasis. *J. Exp. Med.* **188**:1717–1723.
26. van Dam, H., et al. 1998. Autocrine growth and anchorage independence: two complementing Jun-controlled genetic programs of cellular transformation. *Genes Dev.* **12**:1227–1239.
27. Brown, P.H., Chen, T.K., and Birrer, M.J. 1994. Mechanism of action of a dominant-negative mutant of c-Jun. *Oncogene.* **3**:791–799.
28. Guan, B., Yue, P., Lotan, R., and Sun, S.-Y. 2002. Evidence that the human death receptor 4 is regulated by activator protein 1. *Oncogene.* **21**:3121–3129.
29. Bossy-Wetzel, E., Bakiri, L., and Yaniv, M. 1997. Induction of apoptosis by the transcription factor c-Jun. *EMBO J.* **16**:1695–1709.
30. Behrens, A., Sibilia, M., and Wagner, E.F. 1999. Amino-terminal phosphorylation of c-Jun regulates stress-induced apoptosis and cellular proliferation. *Nat. Genet.* **3**:326–329.
31. Yoshida, K., et al. 2002. Amino-terminal phosphorylation of c-Jun regulates apoptosis in the retinal ganglion cells by optic nerve transection. *Invest. Ophthalmol. Vis. Sci.* **43**:1631–1635.
32. Ginsberg, D., Hirai, S.I., Pinhasi-Kimhi, O., Yaniv, M., and Oren, M. 1991. Transfected mouse c-Jun can inhibit transformation of primary rat embryo fibroblasts. *Oncogene.* **4**:669–672.